Solar.q_1: A new solar-tracking mechanism based on four-bar linkages

Solar.q_1: A new solar-tracking mechanism based on 4-bar linkages

Giuseppe Quaglia, Simone Luca Maurino
Department of Mechanical and Aerospace Engineering, Politecnico di Torino, Torino, Italy
giuseppe.quaglia@polito.it
simoneluca.maurino@studenti.polito.it

Corresponding author:
Giuseppe Quaglia, Department of Mechanical and Aerospace Engineering, Politecnico di Torino, Torino, Italy
Email: giuseppe.quaglia@polito.it

Abstract

This paper describes the early stages of the design process of a 2-DOF parallel mechanism, based on the use of 4-bar linkages and intended to move photovoltaic panels in order to perform sun tracking.

Primary importance is given to the search for a way to compensate sun-earth's relative motions with two decoupled rotations of the panel. This leads to devise a kinematic structure characterized by a particular arrangement of the revolute axes. At the same time, the structure itself is designed in order to be slender. Subsequently, the fact that during a day the earth's revolution around the sun has negligible effects on the apparent trajectory of the sun, if compared to the rotation around the polar axis, leads to choose a control strategy which, also thanks to the said arrangement of axes, employs only one DOF for most of the daytime. By means of computer simulations is proved that, so doing, are obtained negligible tracking errors. The tracker which employs this strategy has, theoretically, an energy consumption similar to that of 1-DOF solar trackers but a precision similar to that of 2-DOF ones.

Keywords

Solar-tracking mechanisms, 4-bar linkage, sun trajectory, kinematic analysis and simulation.

1. Introduction

In recent decades the use of large scale photovoltaic power stations has grown up quickly in all over the world, and some of these plants, especially the newest, employ solar-tracking mechanisms in order to move the panels. Solar-tracking allows a substantial increase in the input power of the panel (30% to 40% of more daily absorbed energy than with equal surface of fixed panels, see [1]).

In general, the solar power that reaches the surface of a photovoltaic panel is the sum of three components: direct, diffuse and reflected. During a day of clear sky, the most important is the direct, expressed as

$$P_D = I_{DS} \cdot S \cdot \cos\alpha \tag{1}$$

where I_{DS} is the direct solar power at ground level on a 1m^2 surface normal to the sunrays (expressed in W/m^2), S is the surface of the panel and α is the angle between the sunrays direction and the normal to the surface S (this angular misalignment is defined "tracking error"). Hence the purpose of solar-tracking systems is to reduce the tracking error as much as possible, continuously during the daytime. Several studies have been done on this issue, looking for a good mechanism that can be applied to move a photovoltaic panel (see, for instance, [2]-[5], where different design techniques are followed). Examples of some existing solutions can be found in [6]-[10].

The solution proposed here aims to improve some features that in those seem to be undervalued. In summary are proposed:

1. a mechanical structure that is slender and that can be employed at various latitudes without requiring any change on its geometry;
2. a control strategy and axes arrangement oriented to reduce energy consumption of the tracker;
3. cheap actuation systems.

Below, after a basic classification of solar trackers and some useful astronomical considerations, the steps that lead to the new mechanical structure and its kinematic analysis will be described. After that, a control strategy will be outlined.

2. A classification for existing solar-trackers

Solar trackers are mainly composed by:

1. the mechanism that provides the desired mobility to the panel;

2. the actuation system (composed by actuators and transmissions);
3. the control system (composed by various types of sensors and controllers).

The most relevant classification of solar trackers refers to the number of DOF of the mechanism and to the orientation of the rotation axes with respect to the ground. Figure 1 shows a diagram with the principal existing typologies of solar-tracking mechanisms, and their schematic representation is in Figure 2 and Figure 3, but for a more detailed classification of these mechanisms see [1].

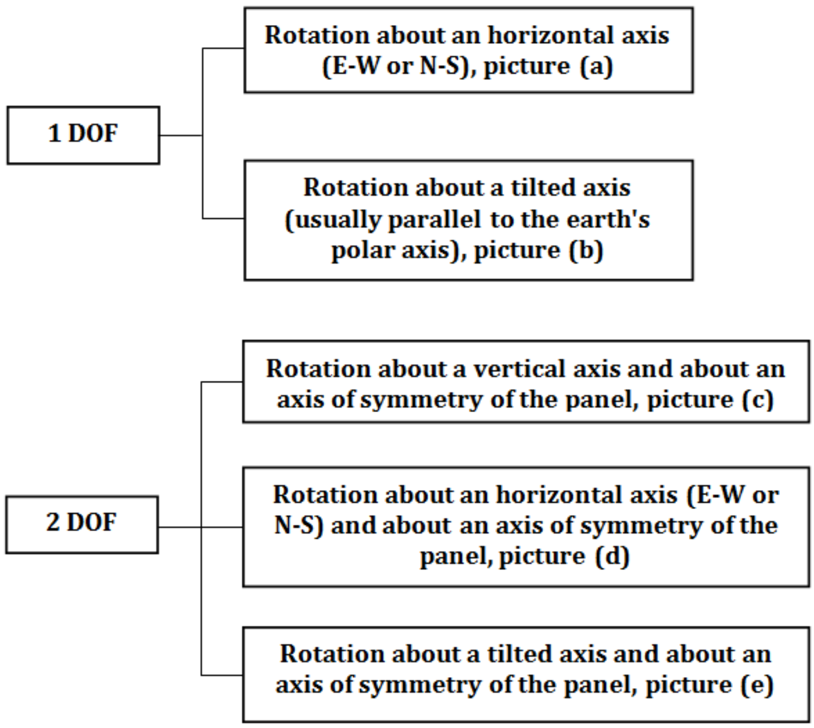

Figure 1. Main typologies of existing solar-tracking mechanisms.

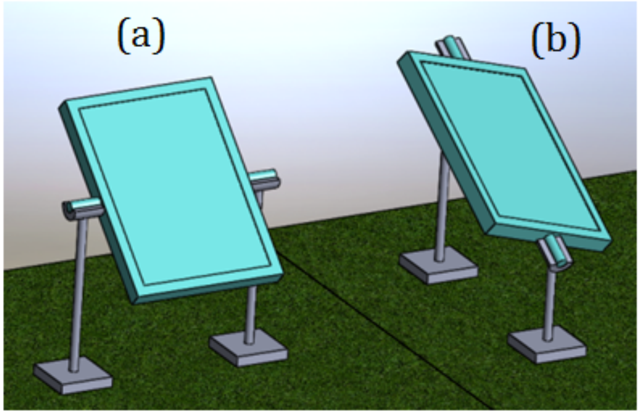

Figure 2. Simplified representation of 1 DOF solar trackers.

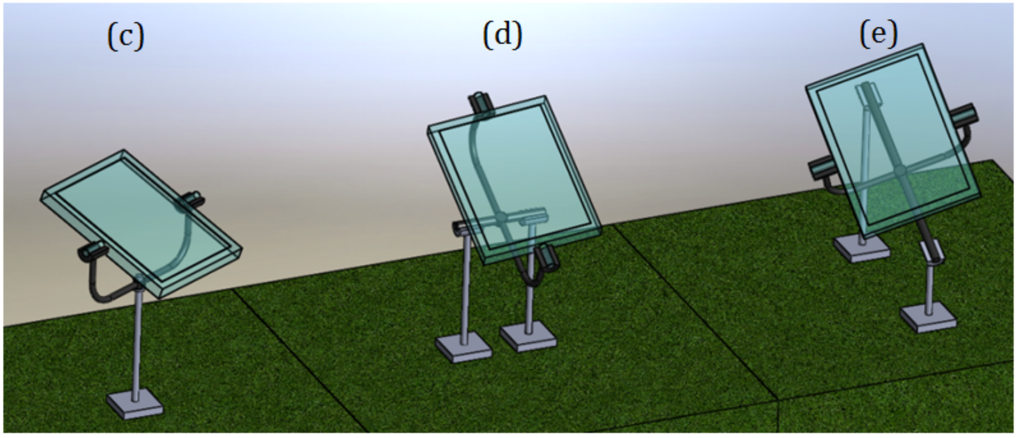

Figure 3. Simplified representation of 2 DOF solar trackers.

Mechanisms with 2 DOF are able to do a theoretically perfect tracking[1], while 1 DOF ones cannot realize always the exact sunrays-panel orthogonality, and so they are at an intermediate level between fixed systems and 2 DOF systems in terms of power increase and of complexity.

Regarding control systems, a solar tracker can be driven according to signals provided by photodetectors, in order to make the panel rotate towards the brightest area of the sky. This area is where the sun is situated if sky is clear, but it can't be if it's a cloudy day. Alternatively, the tracker can be driven in order to follow the sun's apparent trajectory, obtained by astronomical calculations. In mechatronic terms, these cases could be called closed loop and open loop respectively.

According to the classification set out above, the solar tracker that will be described in this paper has got 2 DOF with axes disposed like in case (e) of Figure 3 and follows the solar trajectory regardless of weather conditions (open loop). A key feature of the proposed solution regards the use of the two DOFs: the first is dedicated to the daily solar tracking, while the second is dedicated to fit the system to the seasonal requirements.

---

[1] "Theoretically perfect" means that thanks to this mechanism, the panel is given the possibility to move in all the position in which the tracking error is exactly null, during all the daytime and every day of the year. Hence, if there were an ideal control system and there were no disturbances to the motion (friction and wind for example), the panel could point exactly toward the apparent position of the sun in the sky.

3. Apparent trajectory of the sun and general requirements for kinematics

The earth performs various motions, some easy to observe such as rotation and revolution, and others like precession of equinoxes and precession of apses that are impossible to see to the naked eye for their enormous period. With the purpose of solar-tracking with an accuracy of 1' (1 arcminute) only rotation, revolution and precession of equinoxes can be considered ([11]).

The apparent motion of the sun caused by these real motions of the earth depends on the position of the observer (i.e. the place where the photovoltaic plant is installed). In order to describe the earth-sun relative motion, and thus the required panel's motion, two reference frames fixed on the earth are useful, defined by the axes xyz and $x_0y_0z_0$, (Figure 4,5,6). The origin of the xyz reference frame (Figure 4, 6) coincides with the observer on the surface of earth, the xy plane is parallel to the equatorial one, z-axis is parallel to polar axis and x-axis is tangent to the soil and directed from east to west. In this reference frame the sun position is identified with coordinates declination δ_0 and hour angle θ_0. The former assumes values in the range $[-90°, +90°]$, positive when sun is above the equatorial plane; the latter assumes values in the range $[-180°, +180°]$, positive after midday. Note that in this paper it is assumed that, since the earth-sun distance is much higher than earth's radius, sunrays can be seen as a beam of parallel straight lines, and thus the position of the origin of xyz reference on earth's surface has no influence on the values of δ_0 and θ_0 at a fixed instant.

The reference frame $x_0y_0z_0$ (Figure 5, 6) is a local reference frame, its origin coincides with the observer on the surface of earth, the plane x_0y_0 is tangent to the soil (assumed perfectly plane) and with y_0-axis pointing towards the equator. Hence x_0-axis points towards west if the observer is in northern hemisphere, while points towards east if he is in southern hemisphere. From this reference frame, sun is identified by elevation δ_1 and azimuth δ_2. The first is positive when the sun is above the local horizon and assumes values in the range $[-90°, +90°]$; the second is positive after midday and assumes values in the range $[-180°, +180°]$. For better understanding, the two defined references are compared in Figure 6.

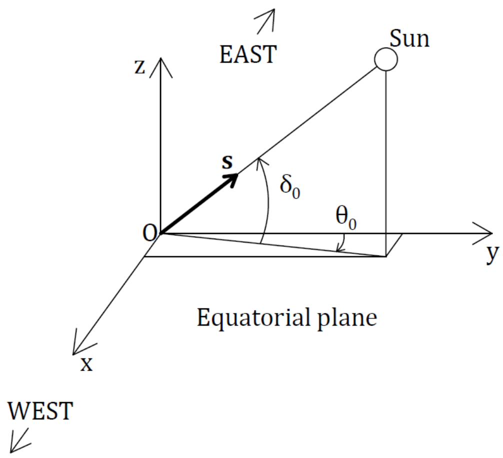

Figure 4. Reference frame xyz used to define the sun position with coordinates declination δ_0 and hour angle θ_0.

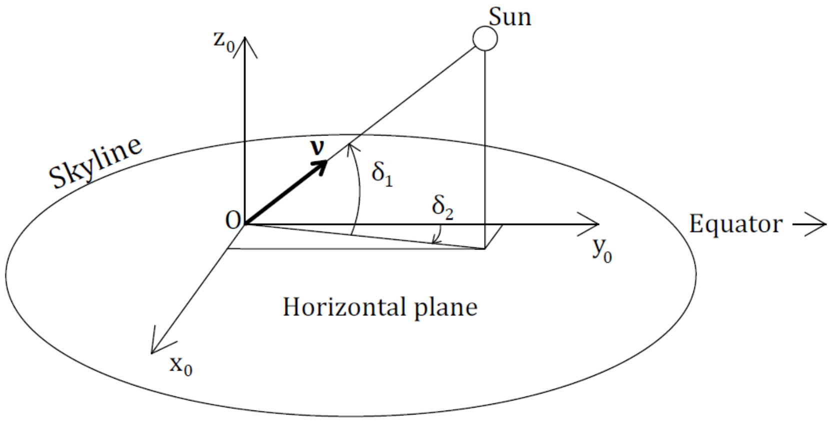

Figure 5. Local reference $x_0y_0z_0$, from which the sun is identified by coordinates elevation δ_1 and azimuth δ_2.

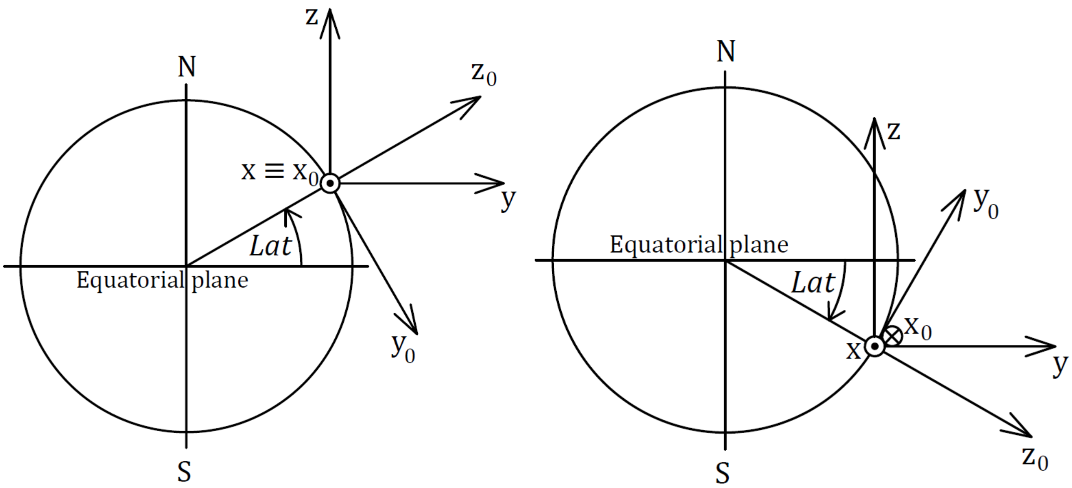

Figure 6. Section of the earth with the two defined references, compared in northern and southern hemisphere (*Lat* means latitude).

The reference xyz allows to determine the sun position in the sky without specifying the latitude of the observer on earth, and so doing calculations are simplified. Here below are reported some excerpts of a more extensive procedure for the calculation of solar coordinates at a generic instant, taken from [11].

The value of θ_0 at a generic instant can be found as

$$\theta_0 = (TVL - TVL_0) \cdot \omega_a \tag{2}$$

where:

1. TVL is the "true local time", the time (expressed in hours) according to which are 12:00 when sun is exactly in south direction (north if the observer is in the southern hemisphere). It is not the time displayed by a common watch near the observer.
2. TVL_0 is the midday instant, valued as 12;
3. ω_a is earth's angular velocity in the rotation motion, valued 15°/hour or $\pi/12$ rad/hour.

TVL is evaluated with the sum of three terms:

$$TVL = GMT + \frac{Long}{\omega_a} + ET \tag{3}$$

where:

1. GMT is the Greenwich mean time at the chosen instant;
2. $Long$ is the local longitude;

3. ET is the equation of time, which takes into account the annual variability of the angular velocity of the earth around the sun (as stated by Kepler's laws) and the tilt of the polar axis with respect to the orbit's plane. In order to evaluate the former, Kepler's equations have to be solved, while for the latter some geometrical considerations (such as the application of Carnot's theorem) are sufficient ([11]).

The value of δ_0 can similarly be determined by means of geometrical considerations and depends only on the earth's position in its trajectory around the sun:

$$\delta_0(t) = -\operatorname{asin}[\sin(\delta_T)\cos(\alpha(t))] \tag{4}$$

where $\delta_T = 23°26'20''$ is the angle between the polar axis and the straight line perpendicular to the orbit's plane (also called obliquity); $\alpha(t)$ is the angular distance around the sun covered by the centre of earth from the last winter solstice to the chosen instant, in its motion of revolution (Figure 7).

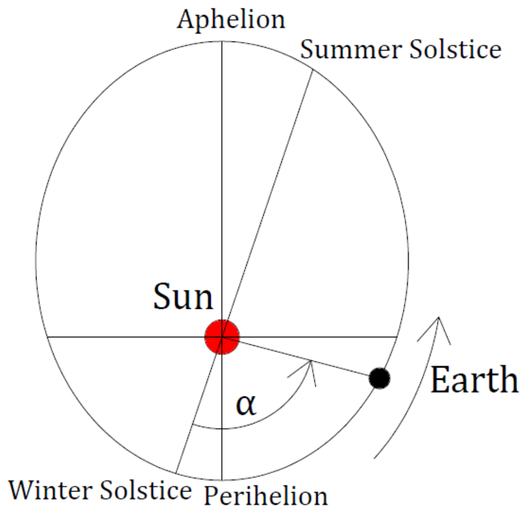

Figure 7. Elliptical trajectory of earth and the above defined angle α.

Hence a unit vector $\vec{s}$ can be defined (Figure 4):

$$\vec{s} = \begin{pmatrix} \cos(\delta_0)\sin(\theta_0) \\ \cos(\delta_0)\cos(\theta_0) \\ \sin(\delta_0) \end{pmatrix} \quad (5)$$

It points toward the real position of the sun from the origin of the xyz coordinate system. However, for the purpose of solar-tracking, the $x_0y_0z_0$ local reference is more practical than xyz and so the new $\vec{s}_0$ unit vector must be defined. It is a vector which points the sun from the origin of the $x_0y_0z_0$ reference and it is obtained by simply applying to $\vec{s}$ a change of reference frame:

$$\vec{s}_0 = \begin{pmatrix} x_0 \\ y_0 \\ z_0 \end{pmatrix} = \boldsymbol{R} \cdot \vec{s} \tag{6}$$

with $\boldsymbol{R}$ a matrix dependent only on the latitude of the observer. It is the rotation matrix to switch from xyz to $x_0y_0z_0$. For places over the equator ($Lat \geq 0°$) it is expressed as

$$\boldsymbol{R} = \begin{bmatrix} 1 & 0 & 0 \\ 0 & \sin(Lat) & -\cos(Lat) \\ 0 & \cos(Lat) & \sin(Lat) \end{bmatrix} \tag{7}$$

While, for places under the equator it is expressed as

$$\boldsymbol{R} = \begin{bmatrix} -1 & 0 & 0 \\ 0 & \sin|Lat| & \cos|Lat| \\ 0 & \cos|Lat| & -\sin|Lat| \end{bmatrix} \tag{8}$$

Unit vector $\vec{s}_0$ can then be decomposed to obtain the angles:

$$\begin{aligned} \delta_1' &= \operatorname{asin}(z_0) \\ \delta_2 &= \operatorname{asin}\left(\frac{x_0}{\cos\delta_1}\right) \end{aligned} \tag{9}$$

While δ_2 is already the desired azimuth, δ_1' is not the correct elevation for it does not take into consideration the light refraction phenomenon operated by the atmosphere. Using Sæmundsson's model of refraction, δ_1 can be obtained adding to δ_1' a specific term Δ dependent on air pressure and temperature ([11]).

The coordinates δ_1 and δ_2 are the requested results, but later will be also useful the unit vector $\vec{v}$:

$$\vec{v} = \begin{pmatrix} \cos(\delta_1)\sin(\delta_2) \\ \cos(\delta_1)\cos(\delta_2) \\ \sin(\delta_1) \end{pmatrix} \tag{10}$$

It points toward the apparent position of the sun, from the origin of the local coordinate system (Figure 5).

The described procedure calculates the elevation and azimuth of the sun in the sky starting from the terrestrial coordinates of the observer, the date and time of Greenwich, temperature and pressure of the air, as it is showed in Figure 8.

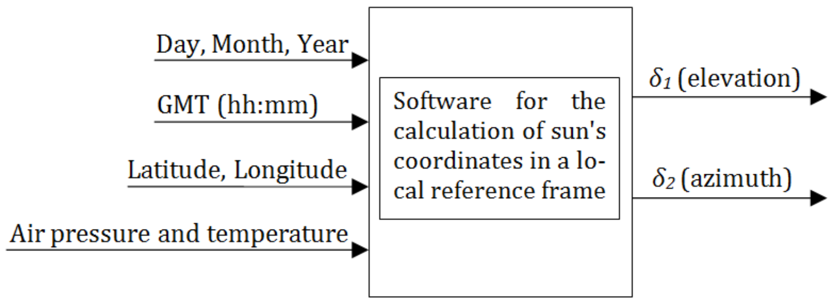

Figure 8. Automated calculus of sun's coordinates.

The software calculates in output the trajectory of the sun in terms of local elevation and azimuth, when a set of time values, from the dawn to the dusk for instance, is used as input. Those values represent the direction in the sky toward which the panel must "look" in order to get an effective solar tracking. Hence, after having designed a suitable kinematic structure and having conducted a kinematic analysis on it, it will be necessary to pass from the target direction's coordinates (δ_1 and δ_2) to the joint coordinates, so as to obtain the panel's trajectory.

In order to introduce the proposed mechanism, some astronomical considerations are useful. Utilizing the concept of inverse kinematics, the hypothesis that there is no light refraction and considering a reference frame fixed on earth, the sun apparently rotates around the polar axis with the opposite angular velocity of that of our planet. This is schematically shown in Figure 9, for an arbitrarily chosen day near to winter solstice.

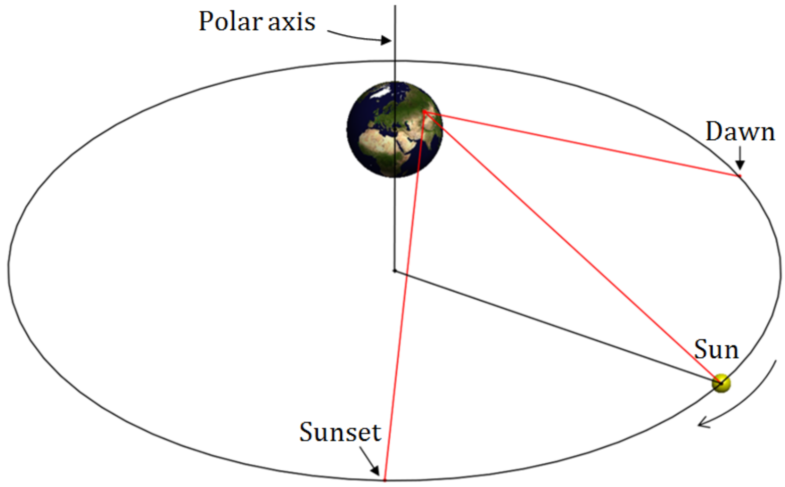

Figure 9. Kinematic inversion of the rotational motion of earth.

In an arbitrary place at about 40° of latitude, for instance, during the entire day the observer can see only the fraction of the solar trajectory which the local skyline permits him (Figure 10). Clearly this statement is true also for any other place on the surface of earth.

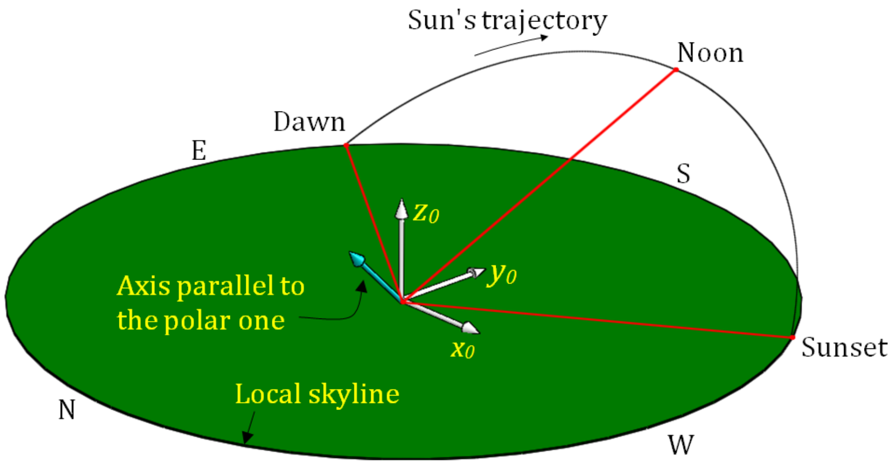

Figure 10. Sun trajectory from dawn to dusk seen in the local $x_0y_0z_0$ reference frame in an arbitrary place at about 40° of latitude during a day near to winter solstice; x_0y_0 plane is tangent to the soil.

Note also that, according to the hypotheses, during that day the unit vector $\vec{v}$ rotates about the axis which is parallel to the polar one and makes a fraction of a conical surface.

In this imaginary case, the plane of the photovoltaic panel, having to be perpendicular to $\vec{v}$ (i.e. to the sunrays), should also rotate about the same axis and thus its solar-tracking mechanism should have only one rotational degree of freedom, that is the rotation about an axis parallel to the polar one.

Since the earth also performs the motion of revolution and precession of equinoxes together with the rotation, the above mentioned circular trajectory is continuously deformed in a way that is barely observable during a day, but very clearly during an entire year. Regarding the revolution, its effect consists in a periodic variation of the width of the interval of azimuth and variation of the maximum elevation reached (i.e. at midday).

As an example, in Figure 11 are shown three sun's trajectories for a place at 45° of latitude.

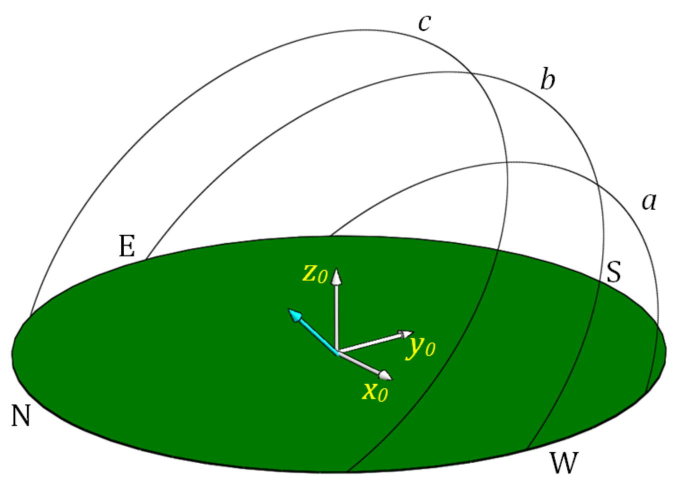

Figure 11. Trajectories of the sun, seen at 45° of latitude at summer solstice (c), winter solstice (a) and equinoxes (b); the fourth unnamed vector indicates the axis parallel to polar one.

While at winter solstice the trajectory is (a) with the lesser azimuth range (from dawn to dusk) and the lower sun's culmination (i.e. the elevation at midday), from December to March the trajectory grows up and at spring equinox is (b). From March to June grows more and more finally reaching the curve (c). Afterward it restarts to decrease passing again in (b) at the autumn equinox and reaches (a) at the new winter solstice.

In Figure 12 are shown the same trajectories, this time seen from a place at the equator.

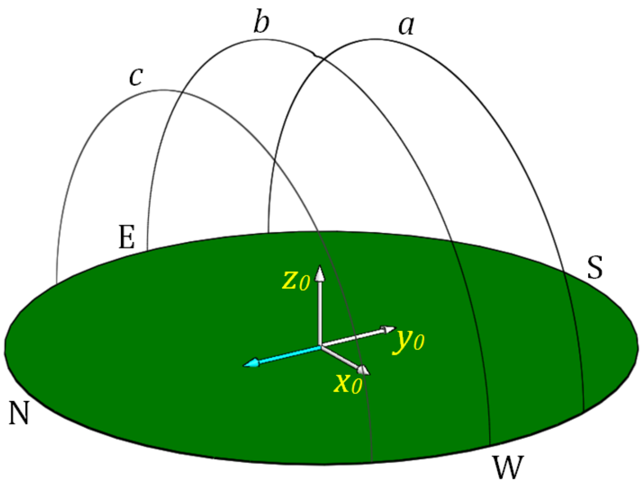

Figure 12. Trajectories of the sun seen at 0° of latitude at summer solstice (c), winter solstice (a) and equinoxes (b); the fourth unnamed vector indicates the axis parallel to polar one.

Seeing these sort of trajectories it's clear that mechanisms using 2 decoupled rotational degrees of freedom are interesting for a precise solar-tracking mechanism. One DOF is required to compensate the motion of daily rotation, and another DOF to compensate the revolution (and for the precession too).

4. A new solar-tracking mechanism

4.1 A simple theoretical solution

Since two decoupled rotations are required, a simple way to obtain them is the use of a universal joint linked between the frame (fixed on the ground) and the panel, as shown in Figure 13.

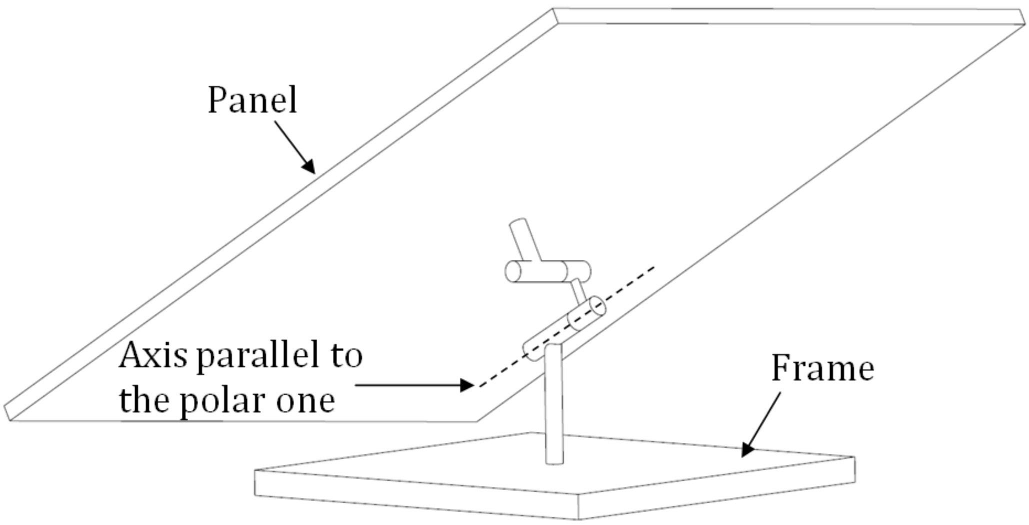

Figure 13. A very simple kinematic chain to move a panel with 2 rotational DOF is constituted by a universal joint.

The first revolute joint (nearest to the ground) has got an axis which is fixed and tilted respect to the ground of an angle equal to the latitude of the chosen location, in order to be parallel to the polar axis. This revolute joint is intended to compensate only earth's rotation about polar axis, as it was requested in the imaginary case seen previously. The second revolute joint has been introduced specially to compensate the motion of revolution about the sun. Note that these two axes cannot be exchanged without losing the univocal correspondence between each of them and the specific motion pattern for which they have been chosen.

From simple considerations about the structural resistance, it is not convenient to realize directly this mechanism as it appears in Figure 13, because, if the panel is large or a group of panels is used (as usually is done in existing 2-DOF solar trackers) the vertical pillar must be sufficiently robust to sustain the weight and the other loads, and thus must be massive. Same goes for the joint itself, which is attached to the panel through a small surface. Therefore, it is interesting to search for a 2-DOF mechanism, which is still based on the kinematic chain of Figure 13, but with a geometry that permits to have a slender structure, still capable to resist the same loads.

4.2 Functional description of the new solution

In Figure 14 and 15 is shown the proposed solution for a solar-tracking mechanism. As can be seen, two parallel 4-bar linkages with crossed levers, provide the first DOF. They move a so-called intermediate platform so as to make a rotation about a translating axis. In particular, the platform rotates about the axis that passes through the cross points of the levers, and this axis translates. Since the frame is tilted respect to the ground of the angle equal to the latitude, that translating axis remains always parallel to the polar one, and thus this motion compensates the earth's rotation only. In Figure 16 are showed the movements of the panel that are allowed by the two 4-bar mechanisms.

Another pair of 4-bar linkages (with uncrossed levers) provides the second DOF. Like in the previous DOF, only the rotational component of the motion is significant, while the translational is secondary.

The choice of 4-bar linkages is derived from the observation that, if their levers are stressed mainly in tension or in compression, they must not be very massive to resist. Hence they concur to the slenderness of the structure. However, being the whole mechanism tilted respect to the ground, a good lateral stiffness is also required and, because of this, cross beams are added.

Thanks to this orientation of the axes, one of the main characteristics of this tracker is that it is applicable at all latitudes without changing the lengths of its links, but only the angle between the base of the first mechanism and the ground. In other terms, it can be argued that all the parts above the frame are independent from the latitude of the geographical location of the plant, and they are adapted to it by a simple rotation respect to the soil.

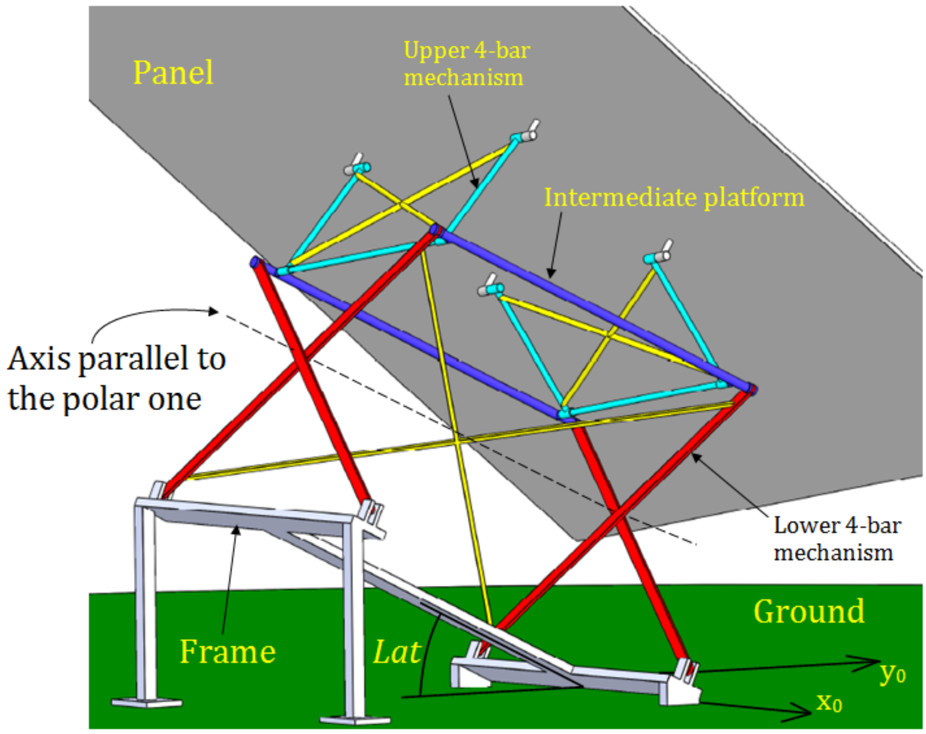

Figure 14. Solution for a 2-DOF solar-tracking mechanism; the two DOFs are provided by 4-bar linkages used in pairs, the first (lower) pair with crossed levers, while the second (upper) pair with uncrossed ones. The frame is tilted respect to the ground of an angle equal to the latitude.

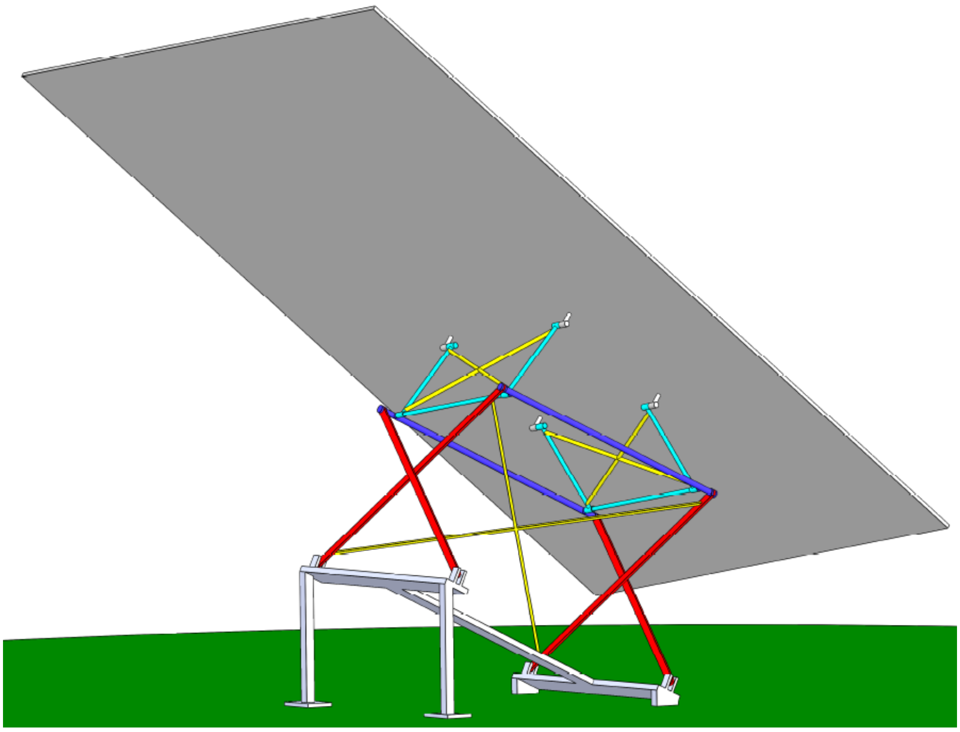

Figure 15. Wide view of the proposed solution.

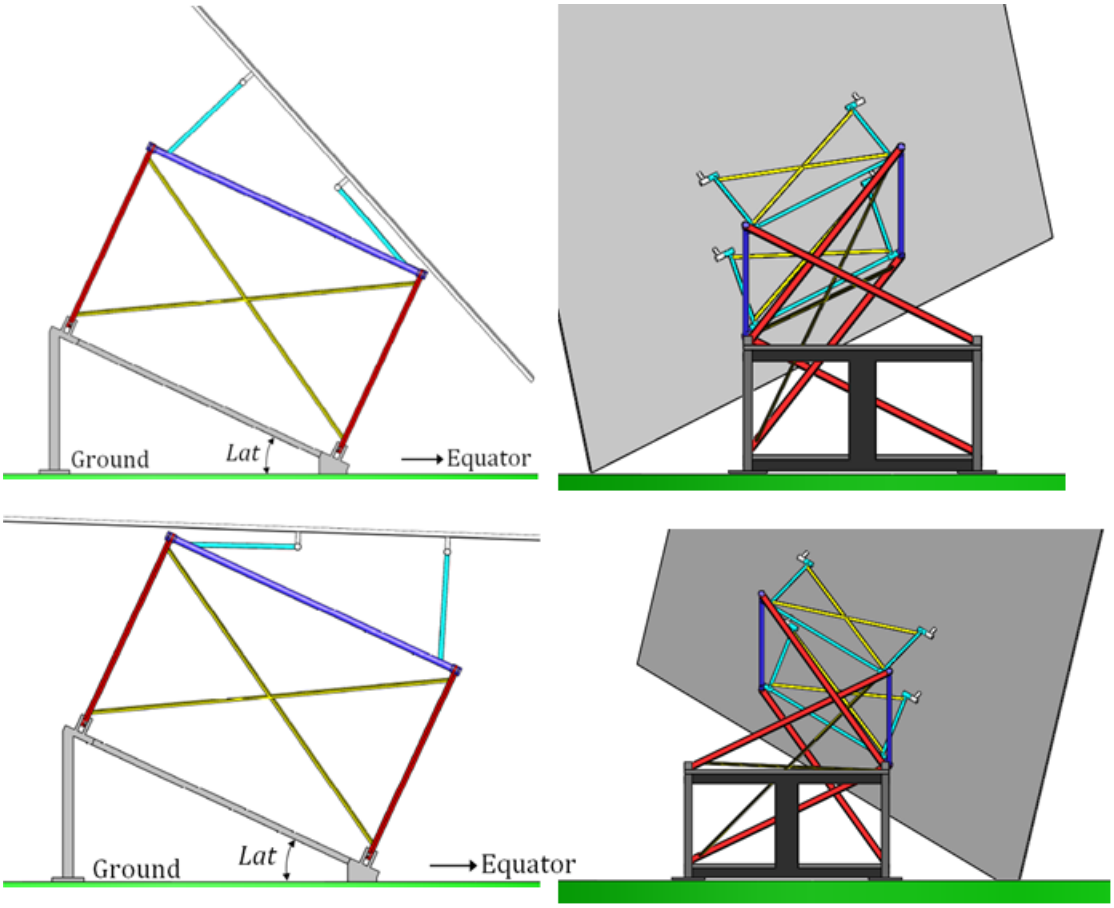

Figure 16. In the left column is shown the movement provided by the upper pair of 4-bar linkages, while in the right column is shown the movement provided by the lower pair.

In Figures 17, 18 are defined the main geometrical parameters for the analysis of 4-bar linkages, while in Figure 19 is shown a schematic representation of the whole mechanism, together with some useful unit vectors which will be used later.

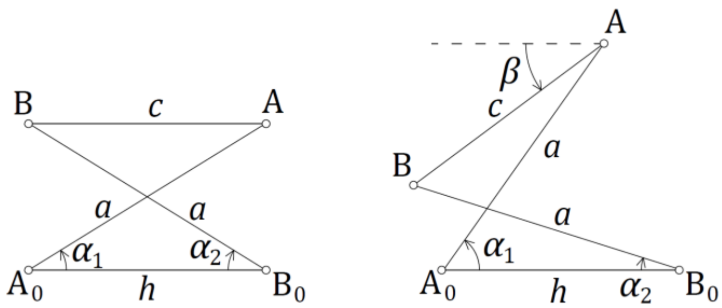

Figure 17. Definition of the main parameters of 4-bar linkages with crossed levers.

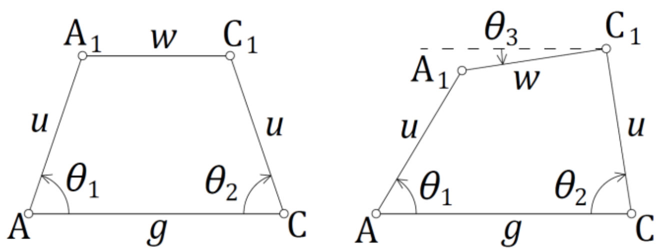

Figure 18. Definition of the main parameters of 4-bar linkages with uncrossed levers.

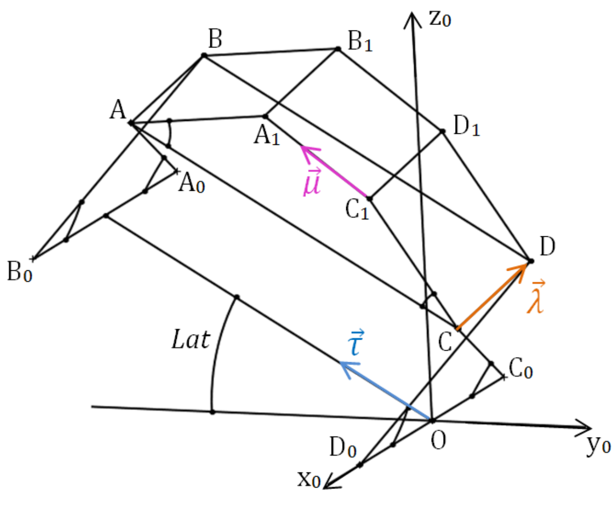

Figure 19. Schematic representation of the mechanism disposed in the local $x_0y_0z_0$ reference frame.

4.3 From sun's coordinates to the configuration of the mechanism

In order to control the position of the sun tracker is necessary to define the relation between the sun's coordinates δ_1 and δ_2 for a generic instant, and the two variables β and θ_3 (Figures 17, 18), that describe the configuration of the mechanism. Note that, as can be seen in Figure 19, the mechanism must be disposed on the ground with that particular orientation respect to the axes of the $x_0y_0z_0$ local reference frame.

Beginning with the definition of the geometry of the 4-bar linkage with crossed levers, the length h (Figure 17) can be chosen arbitrarily (for it constitutes the scale factor of the mechanism), while the lengths a and c must be chosen respecting the following conditions:

$$\begin{cases} a \geq h \\ c \geq \dfrac{1}{2}\left(2a + h - \sqrt{4a^2 - 3h^2}\right) \\ c \leq \dfrac{1}{2}\left(h - a + \sqrt{a^2 + 6ah - 3h^2}\right) \end{cases} \tag{11}$$

If the mechanism satisfy these geometrical conditions (not demonstrated in this paper) the intermediate platform can rotate freely with $\beta \in [-120°, +120°]$ without any collision between the levers of the 4-bar linkage (considered as ideal lines of zero thickness). This range has been chosen in order to be sufficiently wide to track the sun for most of the daytime at any latitude comprised between the arctic circles.

Now, three useful unit vectors must be defined. The first is $\vec{\tau}$:

$$\vec{\tau} = \begin{pmatrix} \tau_1 \\ \tau_2 \\ \tau_3 \end{pmatrix} = \begin{pmatrix} 0 \\ -\cos Lat \\ \sin Lat \end{pmatrix} \tag{12}$$

It is parallel to the polar axis and is contained in the y_0z_0 plane.

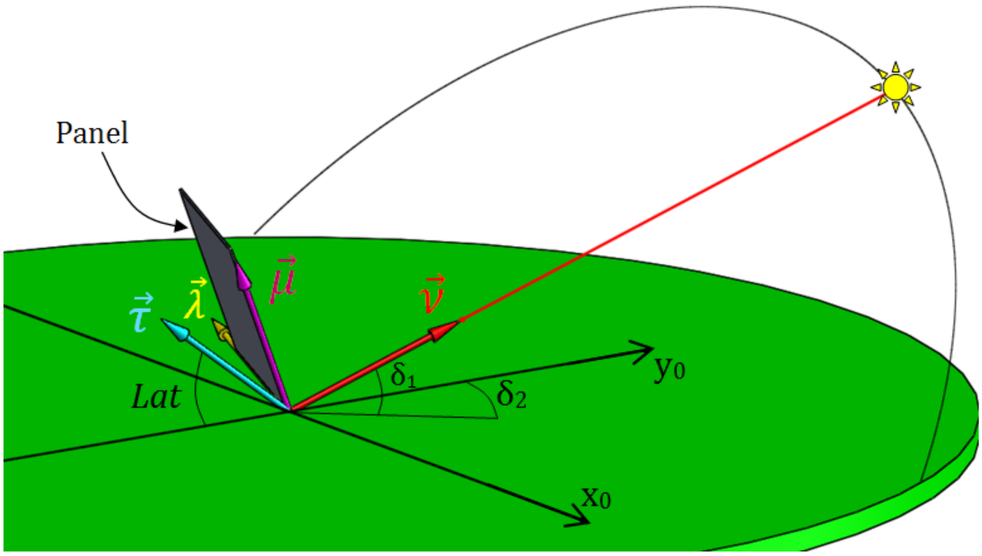

Figure 20. Unit vectors used to define the panel's position.

In order to define an ideal plane which is always perpendicular to $\vec{v}$ (i.e. to sunrays) two others unit vectors are necessary:

$$\vec{\lambda} = \frac{\vec{\tau} \wedge \vec{v}}{|\vec{\tau} \wedge \vec{v}|} \tag{13}$$

$$\vec{\mu} = \frac{\vec{v} \wedge \vec{\lambda}}{|\vec{v} \wedge \vec{\lambda}|} \quad (14)$$

Hence β can be found as

$$\beta = \operatorname{acos}[\vec{\lambda} \cdot (-\vec{\imath})] \quad (15)$$

where $\vec{\imath}$ is the unit vector along the x_0-axis. Note, from Figure 20, that β indicates the rotation of $\vec{\lambda}$ around $\vec{\tau}$.

The other parameter, the angle θ_3, can be determined as

$$\theta_3 = \operatorname{acos}(\vec{\tau} \cdot \vec{\mu}) \quad (16)$$

Once determined the values of β and θ_3, the configuration of the mechanism is known.

4.4 Proposal for a control strategy

As said at the beginning, a particular control strategy for this tracker is proposed here. It consists in moving continuously the tracker in order to compensate the earth's rotation (i.e. varying the β angle of Figure 17) during the daytime, and in executing the other movement (i.e. the variation of the θ_3 angle of Figure 18) only in the mode of one step per day. During this step, which can be accomplished every morning before the daily start-up of the plant, the panel is oriented in a way that the earth's revolution will be exactly compensated in correspondence of the next midday instant. In other terms, the step executed compensates the difference between the sun's positions of the preceding and the subsequent midday.

Intuitively, since the second DOF remains blocked for the rest of the day, the tracking error is not always null (theoretically it vanishes only at midday), but, from results which will be shown later, it can be argued that the tracking error usually remains below 1°. Note that, to achieve this, θ_3 must be calculated as follows:

$$\theta_3 = \mathrm{acos}(\vec{\tau} \cdot \vec{\mu}_{md}) \tag{17}$$

Where $\vec{\mu}_{md}$ is the value of $\vec{\mu}$ at the midday instant of the chosen day.

The advantages of this control strategy are that it allows a certain energy saving, because only one actuator is continuously used for most of the time. Furthermore, the second motion can be very slow and, by means of irreversible transmission system, requires no energy during the rest of the daytime.

4.5 Computer simulations

An algorithm for the computer simulation of the proposed mechanism has been developed, in order to evaluate the theoretical tracking error and to confirm the effectiveness of the suggested control strategy. In its first part, from an arbitrarily chosen time range, it calculates time trends of sun's coordinates according to the procedure described in §3 (and taken from [11]); in the second part it calculates the time trends of β and θ_3, according to the procedure described in §4.3 and §4.4. In the third part it draws the 3D animated scheme of the tracker (like that of Figure 19), and evaluates the elevation and azimuth of the axis perpendicular to the panel (i.e. the target point). By the comparison of these coordinates with δ_1 and δ_2 it can then evaluate the tracking error at every instant (Figure 21).

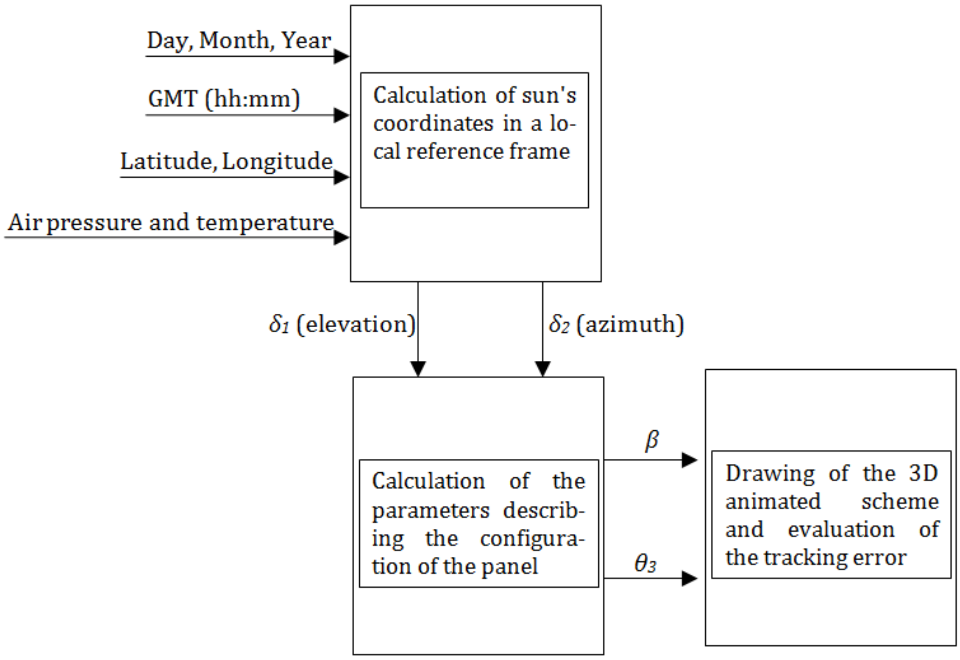

Figure 21. Automated process for the calculation of the parameters β and θ_3.

It must be remembered that neither vibration caused by wind, nor friction have been considered during these simulations, and, as has been noted, the actuation system has not been mentioned yet. These simulations are intended only to prove that the proposed control strategy, together with the particular axes arrangement of the mechanism, can be effective in the ideal case.

Below are showed results of a simulation, whose data are summed up in Table 1:

Table 1. Data which have been assumed during the example test

Latitude	40°
Longitude	0°
Time interval	6 August 2014 5:00÷19:00
Air pressure	1010 hPa
Air temperature	20 °C

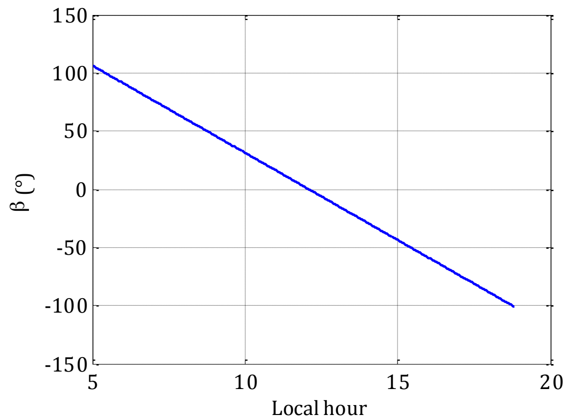

Figure 22. Time trend of the parameter β.

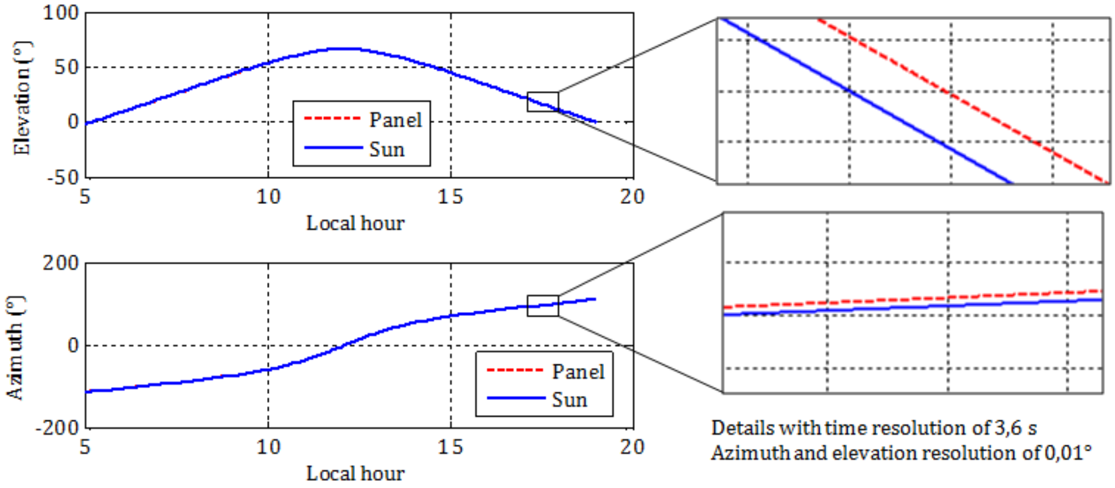

Figure 23. Comparison between time trends of elevation and azimuth of the target point and of the sun.

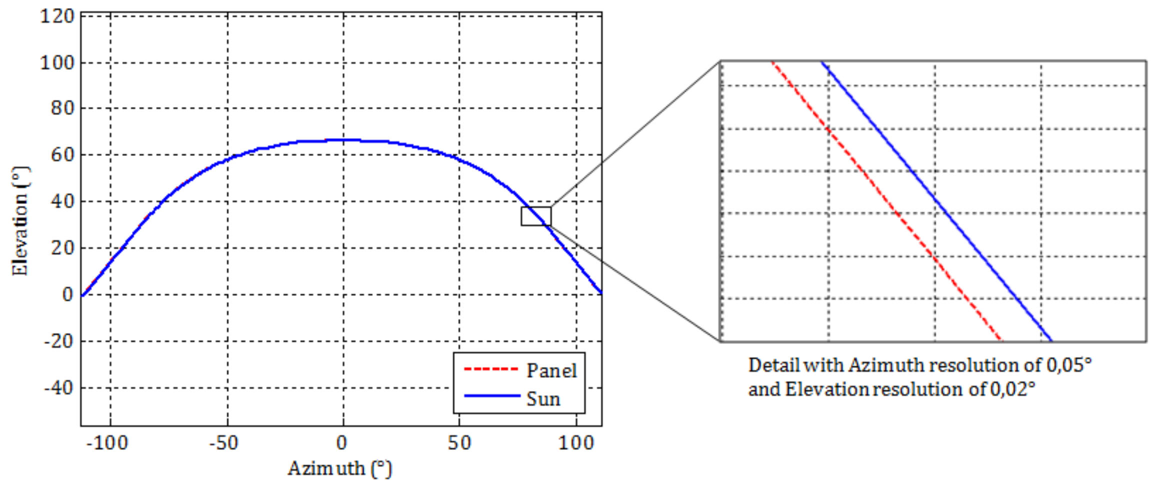

Figure 24. Sun's trajectory in the sky during the chosen daytime compared with the trajectory of the target point.

The following errors are evaluated:

- Maximum elevation error = 0°4'48'';
- Maximum azimuth error = 0°5'24'';
- Maximum tracking error = 0°7'24'';

- Mean elevation error = 0°1'48'';
- Mean azimuth error = 0°2'24'';
- Mean tracking error = 0°2'27'';

Note from Figure 22 that β decreases almost at the angular velocity of earth's rotation, and that the time trends in Figures 23, 24 almost coincide.

A lot of tests like this (for various latitudes and days of the year) provide about the same errors and these, being negligible, confirm that the adopted control strategy is effective. For other examples see Table 2.

Table 2. Tracking errors resulting from various simulations for different places and dates (the time range of analysis is always taken from dawn to sunset).

Date	$\frac{\text{Lat}}{\text{Long}}$	Mean tracking error	Maximum tracking error
14 January 2015	$\frac{25°}{-13°}$	0°01'11''	0°03'32''
26 May 2015	$\frac{-15°}{13°}$	0°01'14''	0°04'10''
2 July 2015	$\frac{54°}{-1°}$	0°01'12''	0°54'47''
12 September2015	$\frac{10°}{0°}$	0°08'06''	0°14'46''
18 November 2015	$\frac{2°}{100°}$	0°02'16''	0°06'42''
28 December 2015	$\frac{-38°}{-73°}$	0°03'09''	0°04'57''

Note that, in the examples, the tracking begins at the dawn and ends at the dusk, but from considerations about the solar power at the ground level it could be necessary shorten the time frame.

Here below is shown the tracker in different moments of the daytime considered.

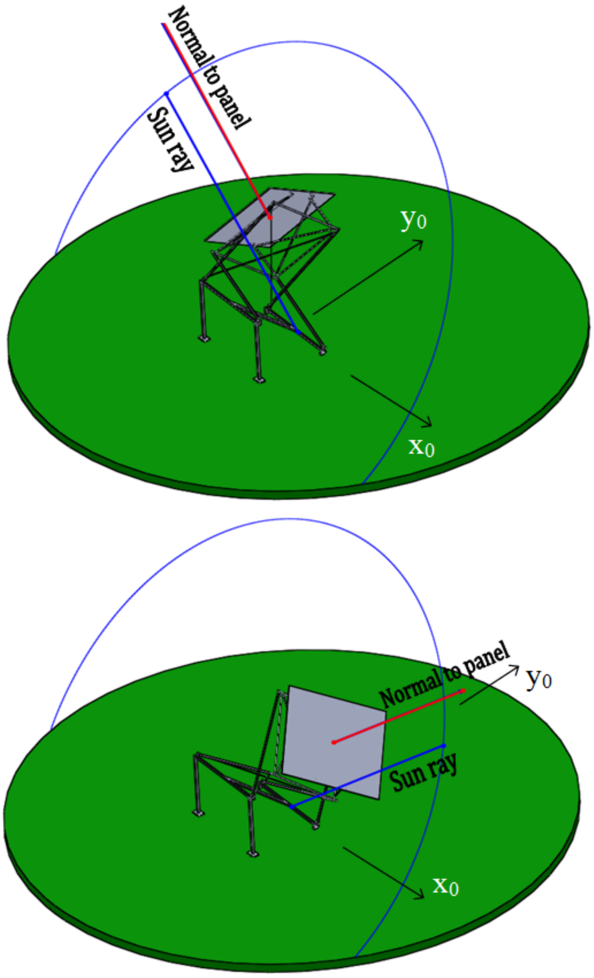

Figure 25. The tracker put on an ideal ground, and oriented towards the sun in two different moments of the daytime.

In Figure 25 it should be noted that the normal to the panel is almost parallel to the sun rays.

4.6 Proposals for the actuation systems

Since the project is at its early stages, here will be described only a few suggestions for the actuation system. It has got transmissions constituted by cables and pulleys, for both the movements which the tracker can perform (Figure 26). This proposal have been chosen keeping in mind the simplicity and low cost of components and easiness to assembly.

For the first DOF, an electric motor and a constant-torque spring are disposed on the frame and fixed to it. Each of them is connected to a sprocket onto which is wrapped the cable, which passes through a pulley and reaches the intermediate platform where is tied. The motor is used to control the angular position (i.e. β) while the spring is used to maintain the cables under tension.

For the second DOF the motor is fixed on the intermediate platform and rotates with it, and the cable moves directly from the sprocket to the panel. A linear spring is used to maintain the cable under tension.

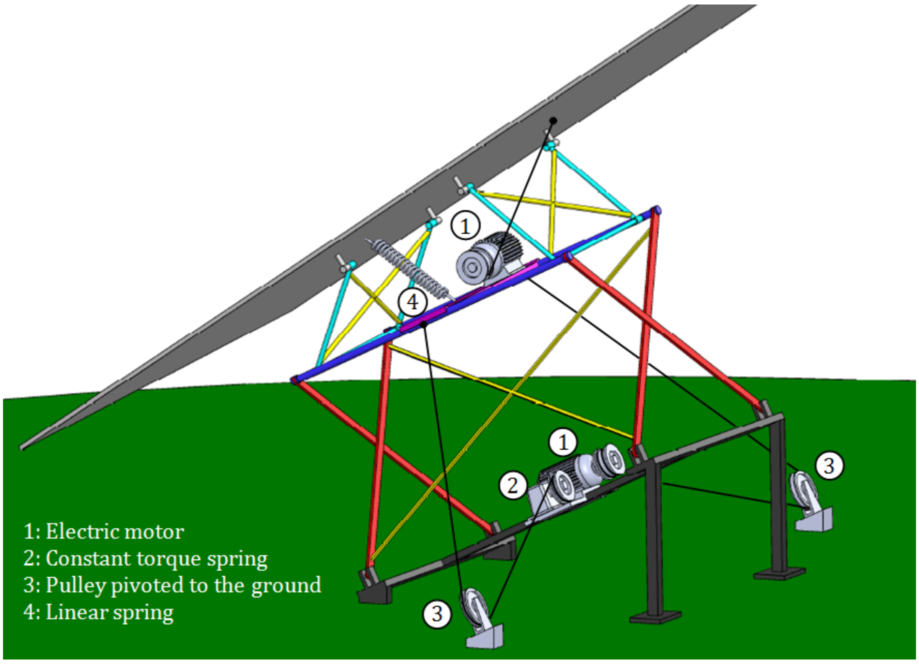

Figure 26. The tracker with the actuation systems, made with electric motors, springs, cables and pulleys.

Note that the motor for the 2nd DOF can have also an automatic brake, so that during the time in which the DOF must be blocked, the motor can simply be turned off and the brake fixes the position of the 2nd DOF, without requiring energy.

On the contrary, the motor for the first DOF rotates continuously in one direction during daytime to move the panel and realize the tracking, but rotates in the opposite direction at night to bring it back to its initial position, in order to restart tracking the next dawn.

A brake can be added in series with the constant torque springs, in order to increase the blocking force, when strong winds appear.

Since cables speed is low, the motors, coupled with gear reducers, can be small, light-weight and cheap. Hence, this actuation system does not burden on the structure.

7. Conclusions

The proposed new solar tracker has a series of advantages that can be here summarized:

1. It is applicable at all latitudes comprised between the arctic circles by simply tilting its mechanism respect to the ground of an angle equal to the latitude, and without modifying anything else of its geometric proportions. However it could be argued that this is not always an advantage because it could be better, for economic or energetic reasons, to optimize the tracker for a geographical region in which it would be installed.
2. Thanks to the particular arrangement of the revolute axes and the control strategy adopted, the tracker behaves like a 1-DOF one for the most of the daytime (because the second DOF is blocked) but, unlike all 1-DOF trackers, provides negligible tracking errors (proved with computer simulations). Hence the energetic supply to the tracker is limited to only one actuator for most of the time, and for a relatively short time per day to both: this implies an energy saving.
3. The mechanical structure is slender. This is achieved thanks to the use of 4-bar linkages and to the use of an actuation system which is oriented to burden on the levers the least possible. A possible critical issue with a slender structure is its stiffness, and detailed studies about this problem are now in development.
4. This project is at his early stage, and many further activities are required in order to design and built a real prototype. In any case the mechanical concept presented in this paper is original and has proved to be very interesting from a kinematic point of view.

Some advantages in terms of control strategy and possible actuation system of the proposed concept are described.

8. References

[1] MOUSAZADEH H, Keyhani A, Javadi A et al. A review of principle and sun-tracking methods for maximizing solar systems output. *Renewable and Sustainable Energy Reviews*, 2009, 19, pp. 1800-1818.

[2] COMSIT M and VIŞA I. Design of the linkages type tracking mechanisms of the solar energy conversion systems by using Multi Body Systems Method. Merlet J-P and Dahan M (eds), *Proceedings of twelfth world congress in mechanism and machine science*, Besancon, France, 2007.

[3] ROLLAND L. Kinematics synthesis of 2 DOF parallel manipulators for solar tracking. *Proceedings of the 21th International Workshop on Robotics in Alpe-Adria-Danube Region (RAAD)*, 2012, ESA, Naples, Italy, pp. 93-100.

[4] ALTUZARRA O, MACHO E, AGINAGA J and PETUYA V. Design of a solar tracking parallel mechanism with low energy consumption. *Proceedings of the Institution of Mechanical Engineers, Part C - Journal of Mechanical Engineering*, 2014, 229 (3), pp. 566-579.

[5] DIACONESCU DV, VIŞA I, VĂTĂŞESCU M, HERMENEAN I, SAULESCU R. Synthesis of a bi-axial tracking linkage with a single actuator. *Proceedings of the 10th IFToMM International Symposium*, 2010, Springer, Oulu, Finland, pp. 617-632.

[6] LUMBRERAS RC. *Directable solar panel systems*. Patent 174295, USA, 2011.

[7] SHERMAN J. *Solar tracking for terrestrial solar arrays with variable start and stop positions*. Patent 0102202, USA 2010.

[8] GRANT T, MORALES TORRES R. *Single-axis solar tracker and solar power installation*. Patent 0073565, USA, 2012.

[9] SCANLON M. *High efficiency counterbalanced dual axis solar tracking array frame system*. Patent 0073161, USA, 2011.

[10] CABANILLAS SALDAÑA J P. *Dual-axis solar tracker*. Patent 8237098, USA, 2012.

[11] BOLLANTI S, DE MEIS D, DI LAZZARO P et al. *Calcolo analitico della posizione del Sole per l'allineamento di impianti solari ed altre applicazioni*. Rapporto tecnico ENEA, 2012.

Appendix

Notation

h, a, c	Main lengths of the 4-bar linkage with crossed links
g, u, w	Main lengths of the 4-bar linkage with uncrossed links

p	Air pressure
R	Rotation matrix to transform from xyz coordinate system to the $x_0y_0z_0$ one
T	Air temperature
$\vec{s}$	Unit vector which points toward the Sun from the origin of xyz
$\vec{s}_0$	Unit vector which points toward the Sun from the origin of $x_0y_0z_0$ but doesn't consider light refraction
x_0, y_0, z_0	Axes of the local reference frame
α	Angle covered by earth around the Sun evaluated from the last Winter Solstice to a chosen instant
α_1, α_2, β	Main angles of the 4-bar linkage with crossed links
δ_0	Declination
δ_1	Elevation
δ_2	Azimuth
δ_1'	Elevation without considering the refraction phenomena
δ_T	Angle between polar axis and the normal to the plane of the revolution's orbit
Δ	Sæmundsson's factor for refraction
θ_0	Hour angle
θ_1, θ_2, θ_3	Main angles of the 4-bar linkage with uncrossed links
$\vec{\lambda}$, $\vec{\mu}$	Unit vectors which define an ideal plane normal to the sunrays (to $\vec{v}$)
$\vec{\mu}_{md}$	Value of $\vec{\mu}$ at midday
$\vec{v}$	Unit vector which points toward the Sun from the origin of $x_0y_0z_0$ (refraction comprised); it indicates the sunrays' direction
$\vec{\tau}$	Unit vector parallel to the polar axis
ω_a	Angular velocity of earth around the polar axis (rotation)

Abbreviations

ET	Equation of Time
GMT	Greenwich mean time
Lat	Latitude
Long	Longitude
TVL	True local time
TVL_0	The same, evaluated at midday (12.00)